frontiers in Materials

ORIGINAL RESEARCH
published: 17 February 2021
doi: 10.3389/fmats.2020.631069

The Influence of Additives on the Rheological and Sedimentary Properties of Magnetorheological Fluid

Xiangcheng Zhang[1], *Xiaotong Liu*[1], *Xiaohui Ruan*[1]*, *Jun Zhao*[1] and *Xinglong Gong*[1,2]

[1]School of Mechanics and Safety Engineering, Zhengzhou University, Zhengzhou, China, [2]CAS Key Laboratory of Mechanical Behavior and Design of Materials, Department of Modern Mechanics, University of Science and Technology of China, Hefei, China

In this research, the influence of additives on the rheological and sedimentary properties of the magnetorheological fluid (MRF) was tested and analyzed. The additives were stearic acid, sodium dodecyl sulfate (SDS), and their mixture, respectively. The MRF was composed of carbonyl iron particle, silicone oil, liquid paraffin, graphite particle, bentonite, stearic acid, and SDS. The results indicated that the rheological properties of the MRF were mainly influenced by the mass fraction of carbonyl iron particle. When the mass fractions of carbonyl iron particle and additive were the same, the shear stress of MRF with stearic acid was larger than that of MRF with SDS, and the maximum increment was 73.81%. When the mass fraction of carbonyl iron particle was 40–50%, the shear stress of MRF increased firstly and then decreased with the increase of the external magnetic flux density. When the mass fraction of carbonyl iron particle was 60–70%, the shear stress of MRF increased firstly and then was stable with the increase of the external magnetic flux density. The results indicated that the sedimentary property of MRF with the mixture was better than that of MRF with the stearic acid and SDS. The settling rate of MRF with the mixture increased 91.53% compared to other additives.

Keywords: MRF, stearic acid, sodium dodecyl sulfate, rheological properties, sedimentary properties

OPEN ACCESS

Edited by:
Miao Yu,
Chongqing University, China

Reviewed by:
Xufeng Dong,
Dalian University of Technology, China
Yingdan Liu,
Yanshan University, China

***Correspondence:**
Xiaohui Ruan
rxiaohui@zzu.edu.cn

Specialty section:
This article was submitted to Smart Materials, a section of the journal Frontiers in Materials

Received: *19 November 2020*
Accepted: *28 December 2020*
Published: *17 February 2021*

Citation:
Zhang X, Liu X, Ruan X, Zhao J and Gong X (2021) The Influence of Additives on the Rheological and Sedimentary Properties of Magnetorheological Fluid. Front. Mater. 7:631069. doi: 10.3389/fmats.2020.631069

INTRODUCTION

Magnetorheological fluid (MRF) was a kind of smart material whose rheological properties could be controlled by the external magnetic field (Tang and Conrad, 1996). MRF was a stable suspension that was mainly composed of ferromagnetic dispersed particles, liquid carrier, surfactant, and thixotropic agent (Phule, 1998). With the effect of external magnetic field, the distribution of the magnetic particles inside the MRF could be transformed from a disordered state to a chain or column structure within milliseconds. The chain or column structures were along with the direction of the external magnetic field, and the MRF would show the solid-like state at this time. When the magnetic field was removed, the magnetic particles would return to the original disordered state. The rheological properties and apparent viscosity of MRF changed significantly when the magnetic was applied or removed, and the reversible change between the fluid state and the solid-like state was called the magnetorheological effect (Felt et al., 1996; Lee and Jang, 2011). Because of the excellent rheological properties of MRF, MRF had been widely used in various devices, such as MR clutch (Demenko et al., 2009; Olszak et al., 2019), MR brake (Wang and Bi, 2019; Wu et al., 2020), MR damper (Marinică et al., 2016; Kazakov et al., 2017), and MR polishing (Levin and Khudolei, 2018; Xiu et al., 2018). MRF

had great development prospects in many fields, such as fitness equipment, automobile, polishing, and earthquake resistance.

Since the MR device was first designed and researched by Rabinow in 1948 (Rabinow, 1948), MRF had received extensive attention due to its high yield stress (Guo et al., 2014; Esmaeilnezhad et al., 2017). Researchers had carried out a large number of studies on the properties of MRF, including the shear stress, stability, safety, energy consumption, and economy. Researchers found that the properties of the MRF could be affected by many factors, such as temperature (Chooi and Oyadiji, 2005; Rabbani et al., 2015), shape of the magnetic particle (Kim and Choi, 2011; Shah and Choi, 2014), surfactant (López-López et al., 2008; Zhang et al., 2009; Fei et al., 2015; Xu et al., 2015), and magnetic flux density (Tian et al., 2014; Shan et al., 2015). Researches indicated that though the shear yield stress of MRF was large, the sedimentation stability of the MRF was poor, which seriously restricted the application of MRF. When the MRF was left for a period of time, magnetic particles and carrier liquid would be separated. Due to the interaction of various particles and the large density difference between magnetic particles and carrier liquid, MRF became a thermodynamically unstable system. The aggregation and settlement of solid particles were inevitable. Many methods had been carried out to improve the settling stability of MRF, such as changing the shape of magnetic particles (de Vicente et al., 2010; Laherisheth and Upadhyay, 2017), adding thixotropic agents (De Vicente et al., 2003; Xu et al., 2018), and adding surfactants (Lijesh et al., 2016; Wu et al., 2016; Son, 2018). At present, the researchers still cannot achieve perfect improvement of the rheological and settling properties of MRF, so further research is warranted.

In this article, stearic acid, sodium dodecyl sulfate (SDS), and their mixture were used as additives to study their effects on the rheological properties and settling stability of MRF. We hoped that the results would provide suggestions and references for improving the shear stress and settling properties of MRFs.

MATERIALS AND METHODS

We made the MRF used in this article ourselves. The materials included carbonyl iron particle (CI, Type: CN, Germany BASF, average particle size was 4 μm), SDS (Zhengzhou Alfa Chemical Co., Ltd.), mineral oil (Zhengzhou Alfa Chemical Co., Ltd.), bentonite (Zhengzhou Alfa Chemical Co., Ltd.), black lead (Zhengzhou Alfa Chemical Co., Ltd.), silicone oil (Zhengzhou Alfa Chemical Co., Ltd., 100 viscosity), and stearic acid (Zhengzhou Alfa Chemical Co., Ltd.). All the chemical reagents were used without any further treatment.

Firstly, the CI particles were thoroughly mixed with surfactant in proportion. Then, the mixture and 200 ml anhydrous ethanol were added to a beaker, which was put in the water bath at 80°C. The CI particles and the mixture were stirred continuously by a mechanical stirring stick until the anhydrous ethanol evaporated completely to make the wrapping of the surfactant better on the surface. The liquid paraffin, bentonite, black lead, and silicone oil were then added to the beaker, and the mixture was stirred for 30 min to make the mixture homogeneous. After the temperature of the mixture cooled down to room temperature, it was put into a ball mill and ground for 12 h. After that, the mixture was transferred to a sample bottle for subsequent experiments. The mass fraction of the ingredient in the MRF was shown in **Tables 1–3**. The mass fractions of bentonite, liquid paraffin, and black lead in all MRF were 1, 2, and 1%, respectively.

TABLE 1 | The constituent of MRF with SDS.

Sample number	CI	SDS	Silicone oil	Sample number	CI	SDS	Silicone oil
1	40.0	2.0	54.0	9	60.0	2.0	34.0
2		3.0	53.0	10		3.0	33.0
3		4.0	52.0	11		4.0	32.0
4		5.0	51.0	12		5.0	31.0
5	50.0	2.0	44.0	13	70.0	2.0	24.0
6		3.0	43.0	14		3.0	23.0
7		4.0	42.0	15		4.0	22.0
8		5.0	41.0	16		5.0	21.0

The instrument used for testing the rheological properties of MRF was the commercial rheometer (Anton Paar, MCR 302). During the test, 0.3 ml MRF was placed between the upper plate and the lower plate of the rheometer. The gap between the plates was 1 mm, and the temperature was kept at 25°C during the test. The shear rate and the magnetic field density applied to the MRF during the test could be controlled. The sedimentation properties of the MRF were evaluated by recording the scale of the interface between the supernatant and the MRF.

RESULTS

Rheological Properties

The Influence of the Mass Fraction of CI Particles

During the test, the range of shear rate was logarithmically increasing from 0.01 to 100 (1/s) and the magnetic flux density was linearly increasing from 0 to 1.1 T. The gap between the testing plates was 1 mm, and the temperature was 25°C. The shear stress of samples 1–48 varied with the magnetic flux density was shown in **Figure 1**. In **Figure 1**, the mass fractions of CI particles, SDS, stearic acid, and the mixture of SDS and stearic acid were 40–70%, 2–5%, 2–5%, and 0.5% + 0.5–0.8% + 0.8%, respectively. The maximum shear stress of MRF was obtained and shown in **Table 4**.

It could be seen from **Figure 1** and **Table 4** that the shear stress increased with the increasing of the mass fraction of CI particles and the magnetic flux density. This was because that more chains or columns could be formed when the mass fractions of CI increased. When the magnetic flux density increased, the interaction force between the particles became strong. The increasing numbers of chains or columns and the interaction force between the particles could make the MRF bear a larger load, which showed the increase of the shear stress.

From **Figure 1**, it could be seen that the change of shear stress with magnetic flux density could be divided into two stages. In the first stage, the shear stress increased rapidly with the increase of

TABLE 2 | The constituent of MRF with stearic acid.

Sample number	CI	Stearic acid	Silicone oil	Sample number	CI	Stearic acid	Silicone oil
17	40.0	2.0	54.0	25	60.0	2.0	34.0
18		3.0	53.0	26		3.0	33.0
19		4.0	52.0	27		4.0	32.0
20		5.0	51.0	28		5.0	31.0
21	50.0	2.0	44.0	29	70.0	2.0	24.0
22		3.0	43.0	30		3.0	23.0
23		4.0	42.0	31		4.0	22.0
24		5.0	41.0	32		5.0	21.0

TABLE 3 | The constituent of MRF with stearic acid and SDS.

Sample number	CI	Stearic acid	SDS	Silicone oil	Sample number	CI (%)	Stearic acid (%)	SDS (%)	Silicone oil (%)
33	40.0	0.5	0.5	59.0	41	60.0	0.5	0.5	59.0
34		0.6	0.6	58.8	42		0.6	0.6	58.8
35		0.7	0.7	58.6	43		0.7	0.7	58.6
36		0.8	0.8	54.4	44		0.8	0.8	54.4
37	50.0	0.5	0.5	49.0	45	70.0	0.5	0.5	49.0
38		0.6	0.6	48.8	46		0.6	0.6	48.8
39		0.7	0.7	48.6	47		0.7	0.7	48.6
40		0.8	0.8	48.4	48		0.8	0.8	48.4

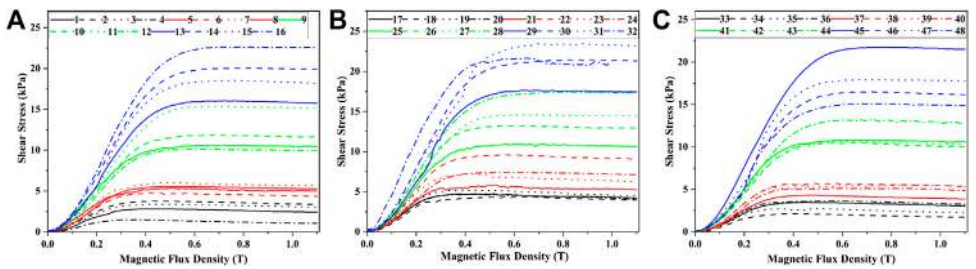

FIGURE 1 | The shear stress varies with the magnetic flux density with different surfactants.

magnetic flux density. This was because the interaction force between the particles increased rapidly at this stage. In the second stage, the shear stress gradually increased and then became stable with the increase of the magnetic flux density. This was because new particle chains were formed under the effect of the magnetic field with the increase of external magnetic flux density, so the shear stress increased gradually. The formation of new grain chains could lead to the increase of the shear stress. When the magnetic flux density increased to 0.4 T, the interaction force between the magnetic particles no longer changed after the magnetization saturation and the structures were no longer changing, which led the shear stress to a stable value.

The Influence of the Surfactant

The curves of the shear stress of MRF vs. the magnetic flux density were shown in **Figure 2**. In **Figure 2A**, the mass fractions of CI particles and additives were 40% and 2%, respectively. Those in **Figures 2B–D** were 50% and 3%, 60% and 4%, and 70% and 5%, respectively.

It could be seen that the shear stress of MRF with stearic acid was higher than that of MRF with SDS. This was because the CI particles in the MRF were gathered and arranged in a chain structure under the effect of the external magnetic field and different surfactants had different effects on the interaction force between CI particles. The stearic acid was coated on the surface of the CI particles and almost had no influence on the viscosity of the carrier liquid. The SDS was dissolved in the carrier liquid, which would make the viscosity of MRF increase. So, SDS would impede the forming of the chain or column structures inside the MRF, which would result in the decreasing of the shear stress.

The Influence of the Shear Rate

The curves of the shear stress of MRF vs. the shear rate were shown in **Figure 3**. In **Figures 3A–C**, the mass fraction of CI

TABLE 4 | Maximum shear stress of MRF.

Sample number	1	2	3	4	5	6	7	8
Maximum shear stress (kPa)	2.42	3.36	3.03	1.06	5.00	4.36	5.69	5.26
Sample number	9	10	11	12	13	14	15	16
Maximum shear stress (kPa)	10.42	11.66	15.13	9.93	15.77	19.90	18.20	22.56
Number	17	18	19	20	21	22	23	24
Maximum shear stress (kPa)	4.20	3.99	4.49	4.04	5.25	9.05	6.27	7.12
Sample number	25	26	27	28	29	30	31	32
Maximum shear stress (kPa)	10.59	12.93	14.42	17.35	17.45	21.31	23.15	21.64
Sample number	33	34	35	36	37	38	39	40
Maximum shear stress (kPa)	3.05	1.71	2.24	3.24	3.87	5.33	5.34	4.88
Sample number	41	42	43	44	45	46	47	48
Maximum shear stress (kPa)	10.62	10.03	10.27	12.85	21.50	16.16	17.77	14.86

particles was 60%. The mass fractions of SDS, stearic acid, and mixture were 2, 2, and 0.5% + 0.5%, respectively. The relationships between the shear stress and shear rate for other samples were similar, so they will not be described in this article for the sake of brevity.

It could be seen from **Figure 3** that the shear stress vs. shear rate curves can be divided into two stages. Firstly, the shear stress first decreased slightly and then increased immediately with the increase of shear rate. Then, the shear stress increases slowly or remained constant with the increase of the shear rate. This was because the magnetic particles would aggregate to form chain or column-like structures parallel to the direction of the external magnetic field when an external magnetic field was applied, which would resist the MRF to flow. In the first stage, when the shear rate was applied to the MRF, the chains between the plates were destroyed and could not be recovered timely, which would lead to the decrease of the shear stress. After that, the particle chains were rebuilt under the effect of the magnetic field, and the phenomenon was that the shear stress increased gradually. In the second stage, new particle chains were formed and, under the effect of magnetic field and chains, would connect to each other to form thick chains under the effect of the shear, so the shear stress increases gradually. At last, the fracture and rebuilt of chains would reach a balance, and the shear stress would reach a stable value. This typical phenomenon can be described by the Bingham model:

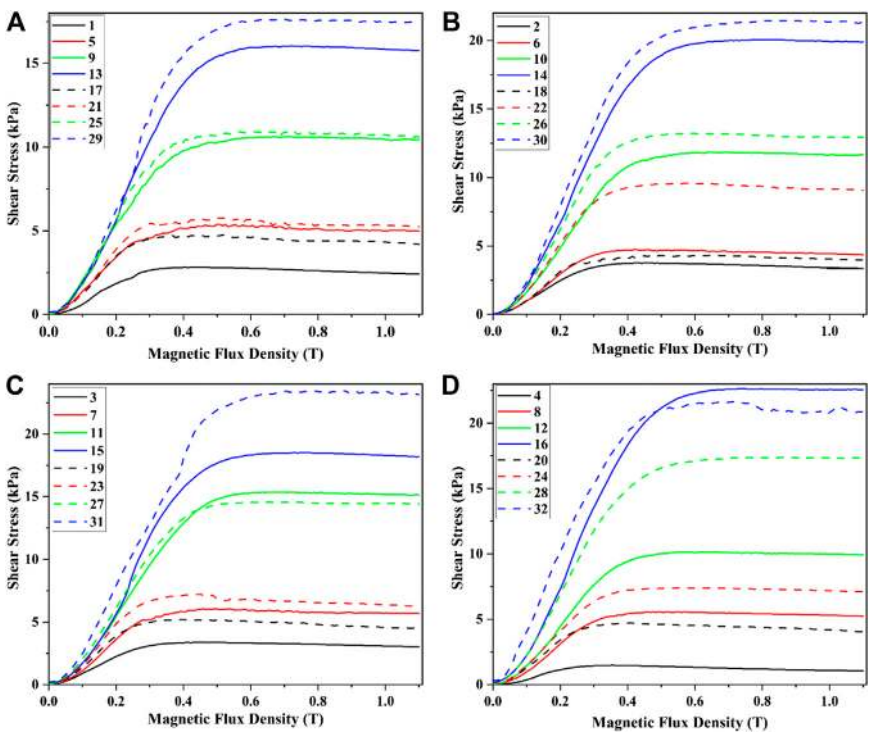

FIGURE 2 | The shear stress varies with the magnetic flux density under different content of surfactants and CI particles.

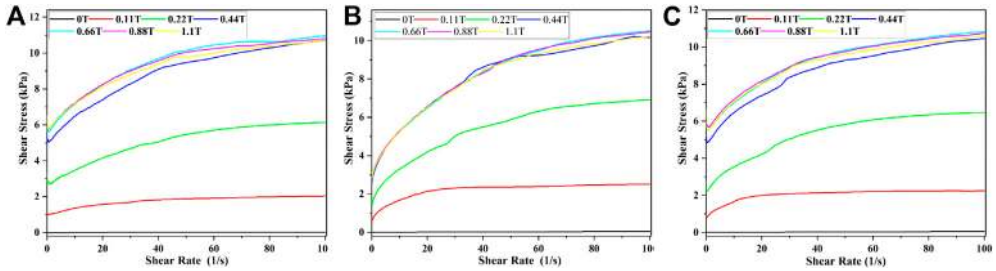

FIGURE 3 | Shear stress varies with shear rate when the mass fraction of CI was 60%, A for SDS, B for stearic acid, and C for mixture.

$$\begin{aligned} \tau &= \tau_y \cdot \mathrm{sign}\dot{\gamma} + \eta\dot{\gamma}, \quad \tau > \tau_y, \\ \dot{\gamma} &= 0, \qquad\qquad \tau \le \tau_y. \end{aligned} \tag{1}$$

In **Eq. 1**, τ_y was the shear yield stress of MRF, determined by the magnetic flux density H (assuming that the field strength was uniform) and the mass fraction of the CI particles, η was the viscosity of MRF, and $\dot{\gamma}$ was the shear rate.

When the mass fraction of CI particle was 40–70% and the mass fraction of SDS was 2%, the experimental and fitting curves of the shear stress *vs*. shear rate of MRF were shown in **Figure 4**. It could be seen that the experimental and fitting results matched well. The yield stress and viscosity of the samples were obtained by fitting the experimental results by **Eq. 1** and were shown in **Figure 5**. It could be seen that the yield stress increased with the increasing of the magnetic flux density and the mass fraction of CI particles. That was because the interaction between the particles increased with the increase of the magnetic flux density and the number of the chain or column structures increased with the increase of the mass fraction of the CI particles. The viscosity of the samples firstly increased and then kept almost constant with the increase of the magnetic flux density. This was because that the interaction between the particles increased with the increase of the magnetic flux density and kept almost constant after the magnetic saturation of the particles. The viscosity of the samples firstly increased and then decreased with the increasing of the mass fraction of CI particles. This was because stratified structures would be formed when the mass fraction of CI particles was very large, which would lead to the decrease of the viscosity.

Settlement Stability

During the test, 10 ml MRF was put into a small measuring cylinder, as shown in **Figure 6**. At the initial time, the liquid level of MRF was level with the scale of 10 ml. The sedimentary

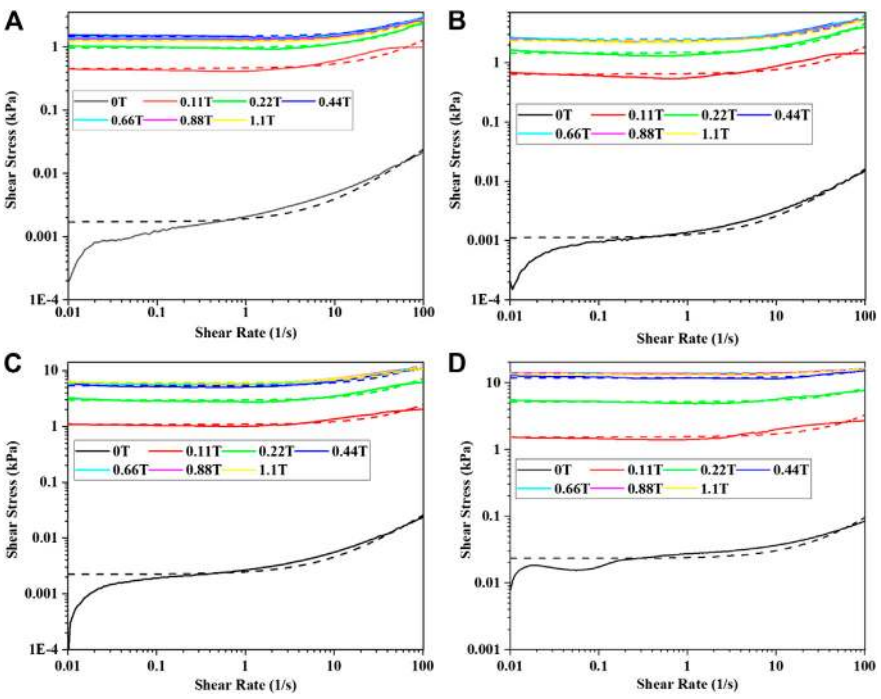

FIGURE 4 | Experimental and fitting curve of shear rate *vs*. shear stress: **(A)** 40%, **(B)** 50%, **(C)** 60%, and **(D)** 70%.

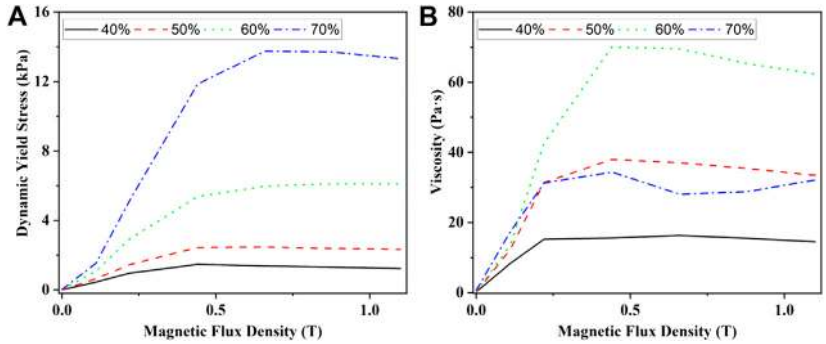

FIGURE 5 | The yield stress and viscosity of the samples.

properties of MRF were evaluated by the method of direct observation. The sedimentation rate was defined as (the height of supernatant/(the height of supernatant + the height of opaque liquid)) *100%, and the formula was as follows:

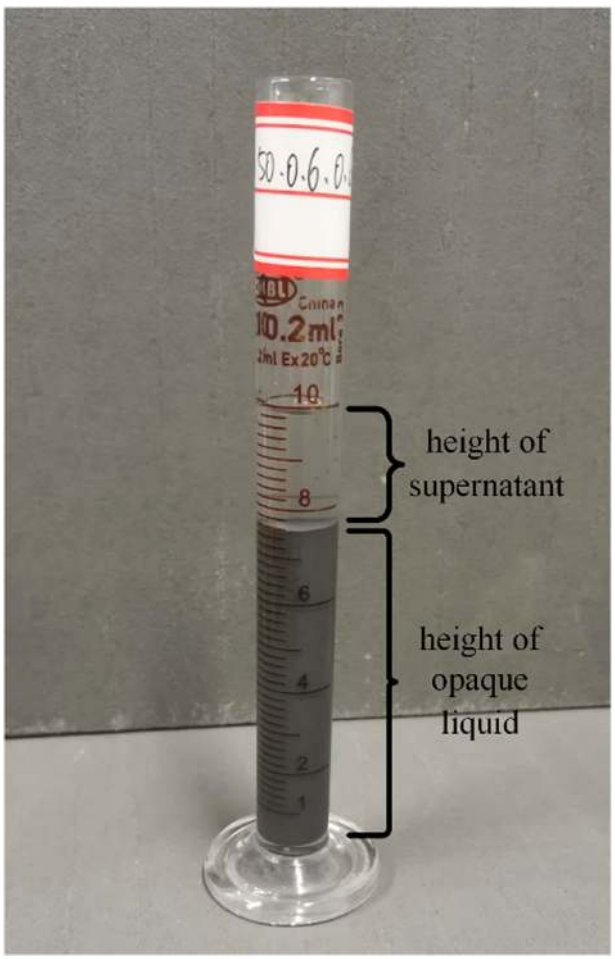

FIGURE 6 | Measuring cylinder.

$$V = \left(\frac{a}{(a+b)}\right) * 100\%. \quad (2)$$

In **Eq. 2**, a was the height of the supernatant and b was the height of the opaque liquid. It could be seen that a smaller sedimentation rate V indicated a better stability property of MRF. The calibration of the supernatant was recorded every 6 h in the first week, every 24 h in the second week, every 72 h in the third week, and every 7 days in the fourth week, until the scale of the supernatant no longer changed. The settling rates of the MRF sample were shown in **Figure 7**, when the mass fractions of CI was 40, 50, and 60% and the surfactant was SDS. Because the fluidity of the MRF was poor when the mass fraction of CI was 70%, it was not concerned here.

It could be seen from **Figure 7** that the sedimentation rate of MRF could be divided into three stages. In the first stage, the sedimentation rate of MRF increased rapidly with the increase of time. In the second stage, the sedimentation rate of MRF increased slowly with the increasr of time. In the third stage, the sedimentation rate MRF gradually tended to be stable. When the mass fraction of SDS was 2%, the increment of sedimentation rate of MRF was the largest when compared to others in the first stage. When the mass fractions of CI particle were 40, 50, and 60%, the MRF with the best settling rate was 6.8, 26.1, and 5%, respectively.

The sedimentation rates of each sample were shown in **Figure 8** when the mass fractions of CI were 40, 50, 60%, and the surfactant was stearic acid. It could be seen from **Figures 8A–C** that the increment of sedimentation rate of MRF was the largest in the first stage when the mass fraction of stearic acid was 2%. When the mass fractions of CI particle were 40, 50, and 60%, the MRF with the best sedimentation rate was 12, 24, and 12%, respectively.

The sedimentation rates of each MRF were shown in **Figure 9** when the mass fraction of CI was 40–60% and the surfactant was mixture. It could be seen from **Figure 9** that the mass fraction of mixture was 0.5%, the increment of sedimentation rate of MRF was the largest in the first stage. When the mass fractions of CI particles were 40, 50, and 60%, the MRF with the best sedimentation rate was 25.8, 0, and 0%, respectively.

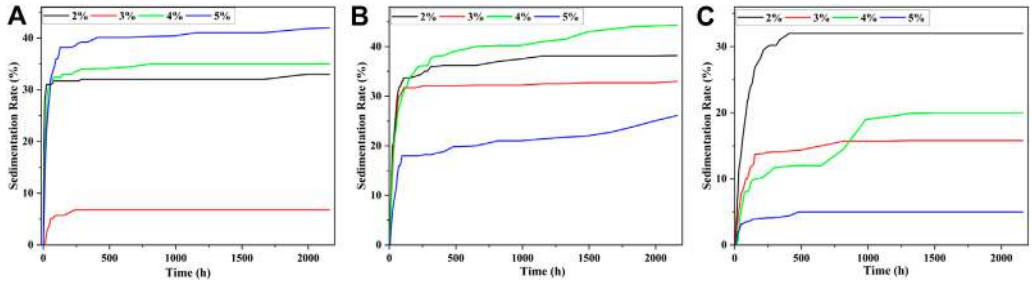

FIGURE 7 | The settling rate when the surfactant is SDS; the mass fraction of CI was **(A)** 40%, **(B)** 50%, and **(C)** 60%.

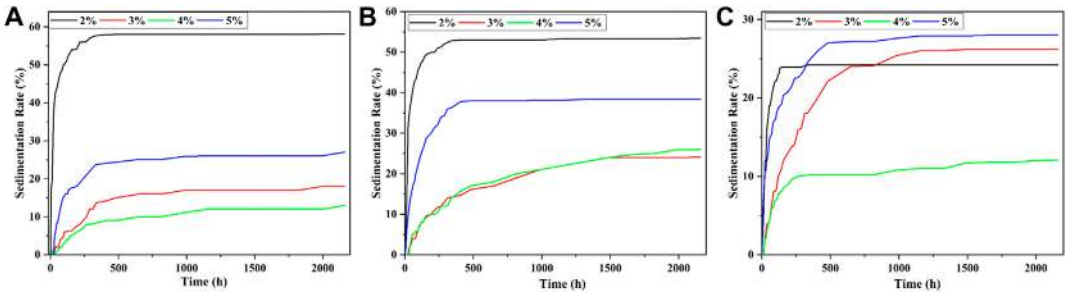

FIGURE 8 | The settling rate when the surfactant is stearic acid; the mass fraction of CI was **(A)** 40%, **(B)** 50%, and **(C)** 60%.

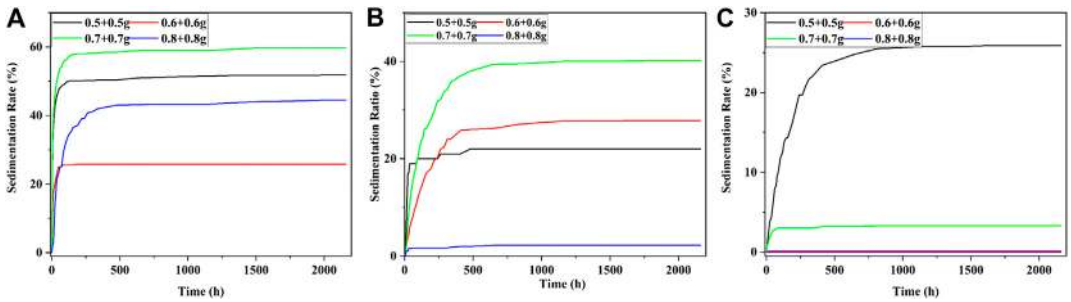

FIGURE 9 | The settling rate when the surfactant was mixture; the mass fraction of CI was **(A)** 40%, **(B)** 50%, and **(C)** 60%.

From **Figure 7** to **Figure 9**, the MRF with the best settling performance for each kind of additives was found and the result was shown in **Figure 10**.

It could be seen from **Figure 10** that the stability of MRF with the mixture was getting better and better with the increase of mass fraction of CI particles. However, when the mass fraction of CI particles was 50%, the stability of MRF decreased when the additives were stearic acid and SDS. When the mass fraction of CI was 60%, the settling stability was mixture > SDS > stearic acid. This was because surfactants had both hydrophilic and lipophilic groups. Hydrophilic groups were usually polar or ionic groups, which were adsorbed on the surface of CI particles. Hydrophobic groups were generally nonpolar groups with long carbon chains, which were dispersed outside CI particles. The long carbon chains among different surfactants were intertwined and repel each other, so they could reduce the aggregation tendency of CI particles and prevent the dispersed particles from aggregation. This kind of coating would change the surface polarity of CI particles, reducing the surface energy and thermodynamic instability and making it easier to disperse in the carrier liquid. So, the settlement problem caused by gravity and settlement stability were improved. The deposition stability of CI with a mass fraction of 50% was lower than that of CI with a mass fraction of 40% due to excess of critical equilibrium concentration. However, the mixture of the two surfactants changed the hydrophilic group and lipophilic group of the surfactant itself. The content of the surfactant never exceeded the critical equilibrium concentration, so the sedimentation

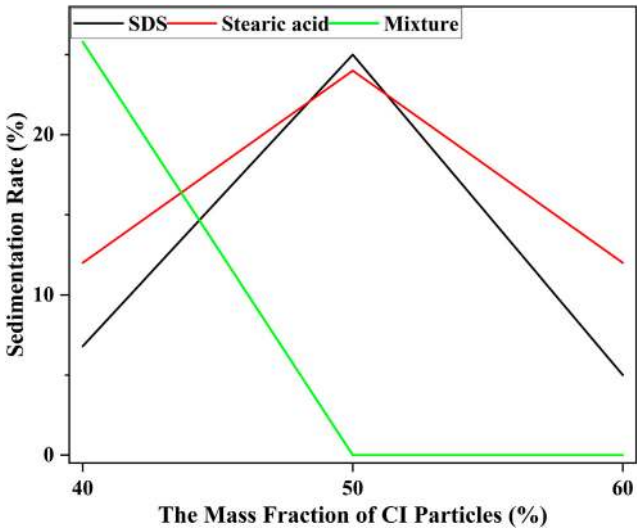

FIGURE 10 | The change of sedimentation rate with the mass fraction of CI particles.

performance would get better with the increase of the amount of surfactant.

CONCLUSION

The rheological properties and sedimentation performance of MRF with different additives had been tested and analyzed in this research. The additives used in this research were SDS, stearic acid, and their mixture. It was found that the rheological properties of MRF were mainly influenced by the mass fraction of CI particles. The shear stress of the samples increased with the increasing of the magnetic flux density and the mass fraction of CI particles. The shear stress of the samples with stearic acid was higher than that of the MRF with SDS when the mass fractions of CI particles and surfactant were equal. When the mass fraction of CI particles was 40 and 50%, the shear stress increased firstly and then decreased with the increase of magnetic flux density. When the mass fraction of CI particles was 60 and 70%, the shear stress increased firstly and then tended to be stable with the increase of magnetic flux density. The relationship between the shear stress and the shear rate could be described by the Bingham model. The yield stress increased with the increasing of the magnetic flux density and the mass fraction of CI particles. The viscosity of the samples firstly increased and then decreased with the increase of the mass fraction of CI particles. The settling stability of the MRF with the mixture of stearic acid and SDS was better than that of the MRF with other additives.

DATA AVAILABILITY STATEMENT

The original contributions presented in the study are included in the article/Supplementary Material; further inquiries can be directed to the corresponding author.

AUTHOR CONTRIBUTIONS

All authors listed have made a substantial, direct, and intellectual contribution to the work and approved it for publication.

FUNDING

Financial support for this research was provided by the National Natural Science Foundation of China (12002317 and 51408555), National Key R&D Program of China (2016YFE0125600), and Program for Changjiang Scholars and Innovative Research Team, University of Minister of Education of China (IRT_16R67); these grants are gratefully acknowledged.

REFERENCES

Chooi, W. W., and Oyadiji, S. O. (2005). Characterizing the effect of temperature and magnetic field strengths on the complex shear modulus properties of magnetorheological (MR) fluids. *Int. J. Mod. Phys. B* 19, 1318–1324. doi:10.1142/s0217979205030244

De Vicente, J., López-López, M. T., González-Caballero, F., and Durán, J. D. G. (2003). Rheological study of the stabilization of magnetizable colloidal suspensions by addition of silica nanoparticles. *J. Rheol.* 47, 1093–1109. doi:10.1122/1.1595094

de Vicente, J., Vereda, F., Segovia-Gutiérrez, J. P., del Puerto Morales, M., and Hidalgo-Álvarez, R. (2010). Effect of particle shape in magnetorheology. *J. Rheol.* 54, 1337–1362. doi:10.1122/1.3479045

Demenko, A., Jędryczka, C., Sujka, P., and Szeląg, W. (2009). The influence of magnetic hysteresis on magnetorheological fluid clutch operation. *COMPEL-Int. J. Comput. Math. Electr. Electron. Eng.* 28, 711–721. doi:10.1108/compel.2009.17428caa.001

Esmaeilnezhad, E., Choi, H. J., Schaffie, M., Gholizadeh, M., Ranjbar, M., and Kwon, S. H. (2017). Rheological analysis of magnetite added carbonyl iron based magnetorheological fluid. *J. Magn. Magn. Mater.* 444, 161–167. doi:10.1016/j.jmmm.2017.08.023

Fei, C., Zuzhi, T., and Xiangfan, W. (2015). Novel process to prepare high-performance magnetorheological fluid based on surfactants compounding. *Mater. Manuf. Process.* 30, 210–215. doi:10.1080/10426914.2014.892967

Felt, D. W., Hagenbuchle, M., Liu, J., and Richard, J. (1996). Rheology of a magnetorheological fluid. *J. Intell. Mater. Syst. Struct.* 7, 589–593. doi:10.1177/1045389x9600700522

Guo, C.-w., Chen, F., Meng, Q.-r., and Dong, Z.-x. (2014). Yield shear stress model of magnetorheological fluids based on exponential distribution. *J. Magn. Magn. Mater.* 360, 174–177. doi:10.1016/j.jmmm.2014.02.040

Kazakov, Y. B., Morozov, N. A., and Nesterov, S. A. (2017). Development of models of the magnetorheological fluid damper. *J. Magn. Magn. Mater.* 431, 269–272. doi:10.1016/j.jmmm.2016.10.006

Kim, J. E., and Choi, H. J. (2011). Magnetic carbonyl iron particle dispersed in viscoelastic fluid and its magnetorheological property. *IEEE Trans. Magn.* 47, 3173–3176. doi:10.1109/tmag.2011.2156396

Laherisheth, Z., and Upadhyay, R. V. (2017). Influence of particle shape on the magnetic and steady shear magnetorheological properties of nanoparticle based MR fluids. *Smart Mater. Struct.* 26, 054008. doi:10.1088/1361-665x/aa54a1

Lee, C. H., and Jang, M. G. (2011). Virtual surface characteristics of a tactile display using magneto-rheological fluids. *Sensors* 11, 2845–2856. doi:10.3390/s110302845

Levin, M. L., and Khudolei, A. L. (2018). Heat transfer in the course of magnetorheological polishing. *J. Eng. Phys. Thermophys.* 91, 797–805. doi:10.1007/s10891-018-1802-3

Lijesh, K. P., Muzakkir, S. M., and Hirani, H. (2016). Rheological measurement of redispersibility and settling to analyze the effect of surfactants on MR particles. *Tribol. Mater. Surface Interfac.* 10, 53–62. doi:10.1080/17515831.2015.1132133

López-López, M. T., Kuzhir, P., Bossis, G., and Mingalyov, P. (2008). Preparation of well-dispersed magnetorheological fluids and effect of dispersion on their magnetorheological properties. *Rheol. Acta.* 47, 787–796. doi:10.1007/s00397-008-0271-6

Marinică, O., Susan-Resiga, D., Bălănean, F., Vizman, D., Socoliuc, V., and Vékás, L. (2016). Nano-micro composite magnetic fluids: magnetic and magnetorheological evaluation for rotating seal and vibration damper applications. *J. Magn. Magn. Mater.* 406, 134–143. doi:10.1016/j.jmmm.2015.12.095

Olszak, A., Osowski, K., Kesy, Z., and Kesy, A. (2019). Investigation of hydrodynamic clutch with a magnetorheological fluid. *J. Intell. Mater. Syst. Struct.* 30, 155–168. doi:10.1177/1045389x18803463

Phule, P. P. (1998). Synthesis of novel magnetorheological fluids. *MRS Bull.* 23, 23–25. doi:10.1557/s0883769400030773

Rabbani, Y., Ashtiani, M., and Hashemabadi, S. H. (2015). An experimental study on the effects of temperature and magnetic field strength on the magnetorheological fluid stability and MR effect. *Soft Matter.* 11, 4453–4460. doi:10.1039/c5sm00625b

Rabinow, J. (1948). The magnetic fluid clutch. *Electr. Eng.* 67, 1167. doi:10.1109/ee.1948.6444497

Shah, K., and Choi, S.-B. (2014). The influence of particle size on the rheological properties of plate-like iron particle based magnetorheological fluids. *Smart Mater. Struct.* 24, 015004. doi:10.1088/0964-1726/24/1/015004

Shan, L., Chen, K., Zhou, M., Zhang, X., Meng, Y., and Tian, Y. (2015). Shear history effect of magnetorheological fluids. *Smart Mater. Struct.* 24, 105030. doi:10.1088/0964-1726/24/10/105030

Son, K. J. (2018). A discrete element model for the influence of surfactants on sedimentation characteristics of magnetorheological fluids. *Korea Aust. Rheol. J.* 30, 29–39. doi:10.1007/s13367-018-0004-z

Tang, X., and Conrad, H. (1996). Quasistatic measurements on a magnetorheological fluid. *J. Rheol.* 40, 1167–1178. doi:10.1122/1.550779

Tian, Y., Chen, K., Shan, L., Zhang, X., and Meng, Y. (2014). Unexpected shear strength change in magnetorheological fluids. *Apl. Mater.* 2, 096102. doi:10.1063/1.4894237

Wang, H., and Bi, C. (2019). Study of a magnetorheological brake under compression-shear mode. *Smart Mater. Struct.* 29, 017001. doi:10.1088/1361-665x/ab5162

Wu, J., Hu, H., Li, Q., Wang, S., and Liang, J. (2020). Simulation and experimental investigation of a multi-pole multi-layer magnetorheological brake with superimposed magnetic fields. *Mechatronics* 65, 102314. doi:10.1016/j.mechatronics.2019.102314

Wu, X., Xiao, X., Tian, Z., and Chen, F. (2016). Study on the preparation process and properties of magnetorheological fluid treated by compounding surfactants. *Jpn. Mag.* 21, 229–234. doi:10.4283/jmag.2016.21.2.229

Xiu, S., Wang, R., Sun, B., Ma, L., and Song, W. (2018). Preparation and experiment of magnetorheological polishing fluid in reciprocating magnetorheological polishing process. *J. Intell. Mater. Syst. Struct.* 29, 125–136. doi:10.1177/1045389x17698247

Xu, J., Li, J., and Cao, J. (2018). Effects of fumed silica weight fraction on rheological properties of magnetorheological polishing fluids. *Colloid Polym. Sci.* 296, 1145–1156. doi:10.1007/s00396-018-4332-9

Xu, Z.-D., Guo, W.-Y., and Chen, B.-B. (2015). Preparation, property tests, and limited chain model of magnetorheological fluid. *J. Mater. Civ. Eng.* 27, 04014229. doi:10.1061/(asce)mt.1943-5533.0001190

Zhang, J. Q., Zhang, J., and Jing, Q. (2009). Effect of seven different additives on the properties of MR fluids. *J. Phys.: Conf. Ser.* 149, 012086. doi:10.1088/1742-6596/149/1/012086

Conflict of Interest: The authors declare that the research was conducted in the absence of any commercial or financial relationships that could be construed as a potential conflict of interest.